Dark-Bright Discrete Solitons: A Numerical Study of Existence, Stability and Dynamics

A. Álvarez [a], J. Cuevas [b,1], F.R. Romero [a], P.G. Kevrekidis [c]

[a] *Grupo de Física No Lineal, Universidad de Sevilla. Área de Física Teórica. Facultad de Física, Avda. Reina Mercedes, s/n, E-41012 Sevilla, Spain*

[b] *Grupo de Física No Lineal, Universidad de Sevilla. Departamento de Física Aplicada I.*
Escuela Politécnica Superior, C/ Virgen de África, 7, E-41011 Sevilla, Spain

[c] *Department of Mathematics and Statistics, University of Massachusetts, Amherst MA 01003-4515, USA*

Abstract

In the present work, we numerically explore the existence and stability properties of different types of configurations of dark-bright solitons, dark-bright soliton pairs and pairs of dark-bright and dark solitons in discrete settings, starting from the anti-continuum limit. We find that while single discrete dark-bright solitons have similar stability properties to discrete dark solitons, their pairs may *only* be stable if the bright components are in phase and are always unstable if the bright components are out of phase. Pairs of dark-bright solitons with dark ones have similar stability properties as individual dark or dark-bright ones. Lastly, we consider collisions between dark-bright solitons and between a dark-bright one and a dark one. Especially in the latter and in the regime where the underlying lattice structure matters, we find a wide range of potential dynamical outcomes depending on the initial soliton speed.

Key words: Solitons, Dark solitons, Discrete Nonlinear Schrödinger equations, Manakov model.

1 Introduction

The setting of multi-component dispersive systems of nonlinear waves is one which has had a significant impact on a variety of areas including the non-

---

[1] Corresponding author. E-mail: jcuevas@us.es

linear optics of fibers and crystals [1] and the recently blossiming area of Bose-Einstein condensates (BECs) in atomic physics [2]. A fascinating example among the complex nonlinear localized structures that can emerge in such settings consists of the so-called symbiotic solitons. These are waveforms that would *not* otherwise exist in unary systems, but are nevertheless supported in multi-component ones, precisely because of the inter-species interaction (be they atomic species in BEC or different frequencies, polarizations or other optical "species" in nonlinear optics). One of the principal examples of this type consists of the dark-bright (DB) solitons in two-component systems with the self-defocusing nonlinearity. The latter class of nonlinearities is well-known to support dark solitary wave structures [3]. However, in the presence of nonlinear interspecies interactions, these dark solitons form a localized potential which allows the trapping in the form of bound states of bright-soliton-like, density bumps leading to the formation of DB waves.

Remarkably, such DB structures have been experimentally monitored both in nonlinear optics and in atomic physics. They were first experimentally created in photorefractive crystals through the pioneering experiments of [4] and subsequently their interactions were partially monitored in [5] [2]. More recently, the realization of multi-component atomic BECs [7–9] has prompted a number of theoretical investigations of DB waves in the latter setting as well starting with the work of [10], which examined the trapped dynamics of DB solitons in the presence of the parabolic traps relevant to BECs. Subsequently, these structures were also extended to more complex settings such as the spinor three-component system, where dark-dark-bright or bright-bright-dark solitons could arise [11]. More recently, the interaction between such dark-bright solitons [12,13] and their potential higher-dimensional generalizations into symbiotic, so-called, vortex-bright solitons [14] have been also considered. Perhaps more importantly, the experiments of [15] were able to provide the first observations of such DB solitons and their interactions e.g. with another dark soliton. A realization of multiple dark-bright solitons has also emerged in the experiments of [16] and the oscillations of dark-bright solitons in a trap, as well as the interaction between two dark-bright solitons were experimentally monitored in [17].

On the other hand, an area of studies that has also received significant attention both within the realm of nonlinear optics and within that of atomic physics concerns the study of nonlinear dynamical lattices. In these, the "evolution variable" is continuum, while the "spatial variables" are discrete. One of the principal reasons for the growth of this field has been the development of optically induced lattices in photorefractive media, such as Strontium

---

[2] It should be noted that theoretical proposals of symbiotic DB solitons (although in a somewhat different setting than what will be considered below) have existed much earlier and at least since the work of [6].

Barium Niobate (SBN) [18], and their experimental realization [19,20]. As a result, a remarkable set of nonlinear waves has been predicted and experimentally observed; these have now been summarized in a number of reviews [21,22]. In addition, another direction of nonlinear optics that has grown in parallel (and has partially preceded the one above) concerns the intriguing interplay of nonlinearity and discrete diffraction emerging in fabricated Al-GaAs waveguide arrays [23]. The numerous interesting phenomena observed therein including discrete diffraction, Peierls barriers, diffraction management, gap solitons, vector solitons, and modulational instabilities among others have now been summarized e.g. in [24,21,22]. Lastly, over the last decade, nonlinear dynamical lattices have emerged as a theme of interest in BECs since droplets of such condensates can be trapped in periodic optical potentials often referred to as "optical lattices" (see, e.g., [26] and references therein). Among the principal byproducts of these studies have been the manifestation of dynamical instabilities, Bloch oscillations, Landau-Zener tunneling, and gap solitons as has been summarized in the reviews [27,28].

Although, to the best of our knowledge dark-bright solitons have *not* been realized in dynamical lattice settings, all of the relevant ingredients illustrating their experimental tractability are available. Namely, recent nonlinear optical experiments have considered the realization of dark solitons in the presence of self-defocusing nonlinearities of both the Kerr type in AlGaAs waveguide arrays [29] and of the saturable type due to the photovoltaic effect in lithium niobate arrays [30]. On the other hand, vector dynamical lattice systems have also been recently experimentally monitored; see e.g. [31] and the discussion therein.

From the above background, it becomes clear that the investigation of DB waveforms in discrete two-component self-defocusing systems is a timely and relevant theme. Our scope in the present work is to numerically explore this topic and the corresponding existence, stability and collision dynamics of DB states in nonlinear dynamical lattices starting from a well-established limit, namely the anti-continuum one of [32]. The latter has been extremely helpful in deriving properties of bright and dark discrete solitons in both focusing and defocusing lattices, as can be seen in the detailed discusssion of [33]. In what follows, we will see that some of the DB states (such as a single DB soliton or pairs of DB solitons with dark ones) draw significant parallels with previously studied cases such as single-component discrete dark solitons. On the other hand, we will also show that other states such as standing wave pairs of two dark-bright solitons have some surprising properties which defy the single-component intuition. As will be seen the linear stability of such states will be critically affected by the relative phase of the bright components. Lastly, we will examine the collisional dynamics of two DB solitons, as well as that of a DB state with a dark one. The latter will reveal a significant wealth of potential outcomes depending on a single parameter, namely the wave speed.

Our presentation will be structured as follows. In section 2, we present the relevant prototypical model setup in the form of two coupled defocusing discrete nonlinear Schrödinger (DNLS) equations. Then, in section 3, we explore the existence and stability properties of the DB solitons. In section 4, we consider their collisional dynamics. Finally, in section 5, we summarize our findings and present our conclusions.

2 Model Setup

We consider the system of two coupled discrete nonlinear Schrödinger (CDNLS) equations given by [33]:

$$i\dot{U}_n + (g_{11}|U_n|^2 + g_{12}|V_n|^2)U_n + C\Delta U_n = 0$$
$$i\dot{V}_n + (g_{12}|U_n|^2 + g_{22}|V_n|^2)V_n + C\Delta V_n = 0, \tag{1}$$

where Δ is the discrete Laplacian operator$(\Delta U_n = U_{n+1} + U_{n-1} - 2U_n)$.

Our focus in what follows will be on stationary solutions of the system of equations (1). To that effect we use the standard *ansatz*

$$U_n(t) = \exp(-i\Lambda_1 t)u_n \qquad ; \qquad V_n(t) = \exp(-i\Lambda_2 t)v_n, \tag{2}$$

with frequencies (propagation constants in nonlinear optics or chemical potentials in BECs) Λ_1 and Λ_2, and spatial profiles $\{u_n\}$ and $\{v_n\}$. Using (2) in (1), we obtain the system of coupled difference equations

$$\Lambda_1 u_n + (g_{11}|u_n|^2 + g_{12}|v_n|^2)u_n + C\Delta u_n = 0$$
$$\Lambda_2 v_n + (g_{12}|v_n|^2 + g_{22}|v_n|^2)v_n + C\Delta v_n = 0. \tag{3}$$

The anti-continuum (AC) limit of [32] (see also [33]) concerns the case with $C = 0$. In the absence of the potential, the system of Eq. (3) results into a pair of analytically solvable algebraic equations for each site. In what follows, and given the nature of the DB solitons, we will restrict our attention to cases where the first (dark) component is excited and the second (bright) one is not i.e., $u_n = \pm\sqrt{-\Lambda_1/g_{11}}$, $v_n = 0$ (at the tails of the DB soliton) or to ones where the first component is inert and the second one is excited i.e., $u_n = 0$ and $v_n = \pm\sqrt{-\Lambda_2/g_{22}}$. (at the center of the DB soliton). Once an exact solution of the DB type has been constructed at the AC limit, it can be continued (numerically, as well as analytically) for finite values of the coupling C. It

4

is worth remarking that throughout the text, unless otherwise specified, free ends boundary conditions have been used.

A relevant question concerning the solutions at finite values of C is that of dynamical stability. To that effect, we use linear stability analysis to provide a spectral response to this question. The stability is determined in a frame rotating with frequency Λ_1 for $U_n(t)$ and Λ_2 for $V_n(t)$, i.e., we suppose that [34]

$$U_n(t) = \exp(-i\Lambda_1 t)[u_n + \xi_n^{(1)}(t)], \qquad V_n(t) = \exp(-i\Lambda_2 t)[v_n + \xi_n^{(2)}(t)]. \quad (4)$$

The small perturbations $\xi_n^{(k)}(t)$, with $k = 1, 2$, can be expressed as

$$\xi_n^{(1)}(t) = a_n \exp(i\omega t) + b_n \exp(-i\omega^* t), \qquad \xi_n^{(2)}(t) = c_n \exp(i\omega t) + d_n \exp(-i\omega^* t), \quad (5)$$

leading to the linear stability equations

$$\omega \begin{pmatrix} a_n \\ b_n^* \\ c_n \\ d_n^* \end{pmatrix} = \begin{pmatrix} K_{1,n} & g_{11}u_n^2 & g_{12}u_n v_n^* & g_{12}u_n v_n \\ -g_{11}(u_n^2)^* & -K_{1,n} & -g_{12}u_n^* v_n^* & -g_{12}u_n^* v_n \\ g_{12}u_n^* v_n & g_{12}u_n v_n & K_{2,n} & g_{22}v_n^2 \\ -g_{12}u_n^* v_n^* & -g_{12}u_n v_n^* & -g_{22}(v_n^2)^* & -K_{2,n} \end{pmatrix} \begin{pmatrix} a_n \\ b_n^* \\ c_n \\ d_n^* \end{pmatrix} \quad (6)$$

with

$$K_{1,n} = \Lambda_1 + 2g_{11}|u_n|^2 + g_{12}|v_n|^2 + \Delta,$$
$$K_{2,n} = \Lambda_2 + 2g_{22}|v_n|^2 + g_{12}|u_n|^2 + \Delta.$$

More specifically, it can be proved [33] that a solution is spectrally stable if all the ω eigenvalues (the so-called eigenfrequencies of the system) are real numbers. Two type of instabilities are observed in this system: (i) exponential instabilities, represented by a eigenfrequency (ω) pair with zero real part and non-vanishing imaginary part and (ii) oscillatory instabilities, accounted for by a Hamiltonian Hopf bifurcation, and represented by quartets of eigenfrequencies with non-zero real and imaginary parts.

Throughout this paper we have assumed $g_{11} = -0.97$, $g_{22} = -1.03$ and $g_{12} = -1$, chiefly motivated by the experimental discussed interspecies interaction ratios of [7,8]. All the calculations have been performed assuming (without loss of generality) $\Lambda_1 = 1$, and for the frequency $\Lambda_2 > 0$ we have explored the range $\Lambda_2 \in [0, 1.5]$, as representative of the different parametric regimes.

3 Stability properties of dark-bright multi-soliton solutions

3.1 Solutions at the anti-continuous limit

In this subsection, we examine a representative set of structures which are initialized at $C = 0$. In the AC limit, we use the following convenient notation to represent our solutions: by indicating $\tilde{u}_n = \pm 1$, we denote an excited site of $u_n = \pm\sqrt{-\Lambda_1/g_{11}}$, while similarly for the second component $\tilde{v}_n = \pm 1$ is used to denote $v_n = \pm\sqrt{-\Lambda_2/g_{22}}$. In this notation, we have considered the following (AC-limit) solutions as seed points for our numerical continuations:

- Dark-bright one-soliton solutions (DB 1-S).

$$\tilde{u}_n = \text{sgn}(n), \qquad \tilde{v}_n = \delta_{n,0}, \tag{7}$$

  where $\text{sgn}(n)$ denotes the sign of n and it is implied that the solution assumes the value $\tilde{u}_0 = 0$.
- Dark-bright two-soliton solutions (DB 2-S). We have considered, as a representative case, that where the distance between the excited bright spots is of 2 sites:

$$\tilde{u}_n = 1 - \delta_{|n|,1} - 2\delta_{n,0}. \tag{8}$$

  In this setting, we distinguish two configurations for the bright part: the in-phase bright case with

$$\tilde{v}_n = \delta_{n,-1} + \delta_{n,1}, \tag{9}$$

  and the out-of-phase (anti-phase) case with

$$\tilde{v}_n = \delta_{n,-1} - \delta_{n,1}. \tag{10}$$

- Dark-bright and dark two-soliton solutions (DB+D). Again, we have considered that there are two sites separating the vanishing sites of the u_n field, one of which is associated with the dark-bright soliton, while the other is associated with the dark one.

$$\tilde{u}_n = 1 - \delta_{|n|,1} - 2\delta_{n,0}, \qquad \tilde{v}_n = \delta_{n,-1} \tag{11}$$

Figure 1 shows some examples of the profile of the above mentioned configurations.

It is interesting to note that at the AC limit, not only the existence theory is transparent but also the nature of the linearization spectrum. More specifically, notice that all the DB states involve configurations for which $u_n v_n = 0$, hence the above $4N \times 4N$ (where N is the number of lattice sites considered)
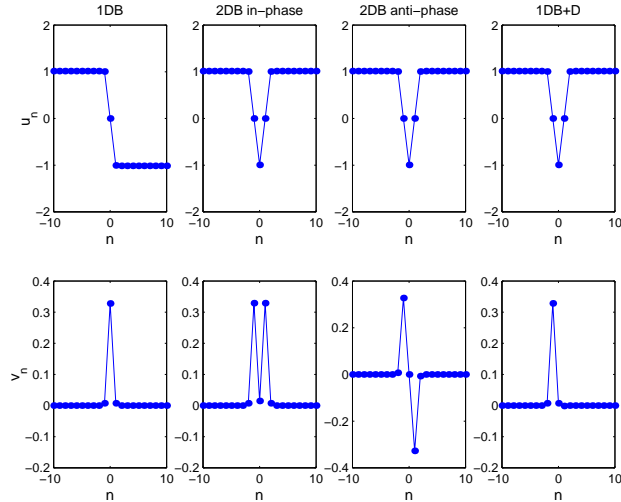
Fig. 1. Profile of the configurations analyzed in the paper. In all cases, $C = 0.02$, $\Lambda_1 = 1$ and $\Lambda_2 = 0.15$.

matrix splits into two diagonal $2N \times 2N$ blocks for each of the components. The background states (away from the DB center) provide each of these components with a spectral dispersion relation of the form:

$$\omega = \pm\sqrt{4C\sin^2(\frac{q}{2})\left(4C\sin^2(\frac{q}{2}) + 2\Lambda_1\right)} \tag{12}$$

between the linearization frequencies ω and wavenumbers q; this relation stems from the dark (first) component. On the other hand, the bright (second) component similarly yields a dispersion relation for the background state (away from the center of the DB)

$$\omega = \pm\left(\frac{g_{12}}{g_{11}}\Lambda_1 - \Lambda_2 + 4C\sin^2(\frac{q}{2})\right) \tag{13}$$

For the excited sites of the dark-bright soliton (where the first component is vanishing i.e., dark and the second component is non-vanishing i.e., bright), we obtain a pair of eigenfrequencies satisfying:

$$\omega = \pm\left(-\frac{g_{12}}{g_{22}}\Lambda_2 + \Lambda_1\right) \tag{14}$$

from the dark component and a pair of zeros from the bright one. The fundamental stability question concerns, of course, the fate of these eigenfrequencies when $C \neq 0$ and is examined systematically in our numerical computations within the following subsection.
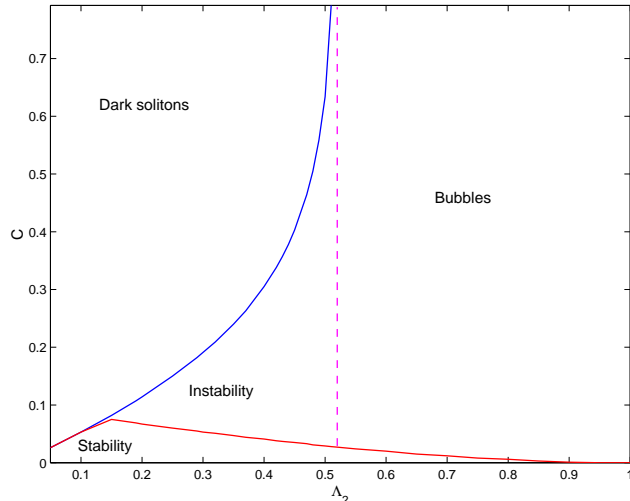
Fig. 2. Existence and stability properties of the dark-bright one-soliton solutions as a function of coupling C and frequency Λ_2, for the case of $\Lambda_1 = 1$.

3.2 Numerical continuations for arbitrary coupling

Having considered the existence and stability properties of the DB waveforms at the AC limit of $C = 0$, we now turn to the case of finite coupling C. In what follows, we examine for the configurations discussed in the previous subsection, the findings pertaining to their existence when a continuation from $C = 0$ is performed, calculating for each solution the eigenfrequencies stemming from the relevant stability problem (6). In every case, $\Lambda_1 = 1$ is fixed whereas Λ_2 is chosen in the interval $[0, 1.5]$.

3.2.1 Dark-bright one-soliton solutions

Three main behaviours are observed separated by the critical values $\Lambda_2 = 0.51$ and $\Lambda_2 = 1$. An overall view for the existence and stability properties of these solutions, as a function of coupling C and frequency Λ_2, is illustrated in Fig. 2.

For $\Lambda_2 \leq 0.51$, stable solutions appear only within a small parametric interval near the AC limit. In this case, past a (Λ_2 dependent) critical point an instability arises due to the collision of a localized eigenmode with the top of the dark component linear mode band, which leads to a Hopf bifurcation. Additionally, the amplitude of the bright spot decreases as C is increased (for fixed Λ_2) vanishing above a critical value of C. For small values of Λ_2, the solution vanishing takes place before the destabilization, implying that the DB soliton is stable in the whole range of C in which it exists with a nontrivial bright component. Fig. 3 (top) shows for a prototypical value of Λ_2 within this parameter range, the dependence of the eigenmode spectrum with respect to C. The figure also features the comparison of the relevant eigenfrequencies with
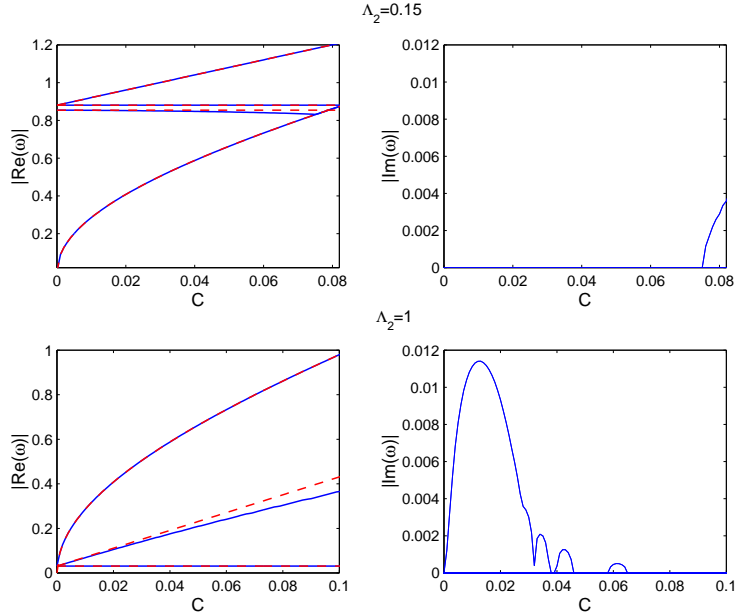
8

Fig. 3. Real part of the relevant spectral eigenfrequencies (left panels) and imaginary part of the eigenfrequency spectrum (right panels) versus C of the DB one-soliton solutions. In both cases, $\Lambda_1 = 1$; the top panels are for $\Lambda_2 = 0.15$, while the bottom ones for $\Lambda_2 = 1$. The dashed lines in the left panels correspond to analytical predictions (12)-(14). Recall that instabilities emerge when $\text{Im}(\omega) \neq 0$.

the analytical predictions (12)-(14) showing an excellent agreement for small C. Recall that per the above analytical predictions there is an internal mode (pertaining to the "dark part" of the DB object) which collides at finite C with the expanding band of phonon spectrum growing away from zero. This fact leads to the observed instability of the DB solitary wave past the relevant critical point in C. When Λ_2 is increased, as it is evident from both Fig. 2 and the bottom panels of Fig. 3, the critical C for the instability emergence tends to 0.

For $\Lambda_2 \in (0.51, 1]$ solutions exist for every value of C. Now, once the localized mode collides with the linear mode band, new parametric regions of stabilization appears as "bubbles" caused by a Hopf bifurcation cascade, as shown in Fig. 4. The size of the instability bubbles decreases and the number of them increases as the number of particles N increases. This is the so called boundary-induced stabilization and is a finite size effect discussed e.g. in [35]. Figure 5 illustrates, as an example, two stability diagrams obtained with $N = 101$ and $N = 10001$. The instability bubbles' size is almost independent of the boundary conditions used, whereas the number of bubbles is independent of them, as shown in Fig. 6. Fig. 3 (bottom) shows the eigenmodes spectrum for an example within this range. This behaviour resembles to that of a dark soliton [35]. Contrary to the above mentioned case, in this parametric regime, there is no vanishing of the bright spot and genuine DB solutions exist for every value of C. Finally, for $\Lambda_2 > 1$, the DB soliton is
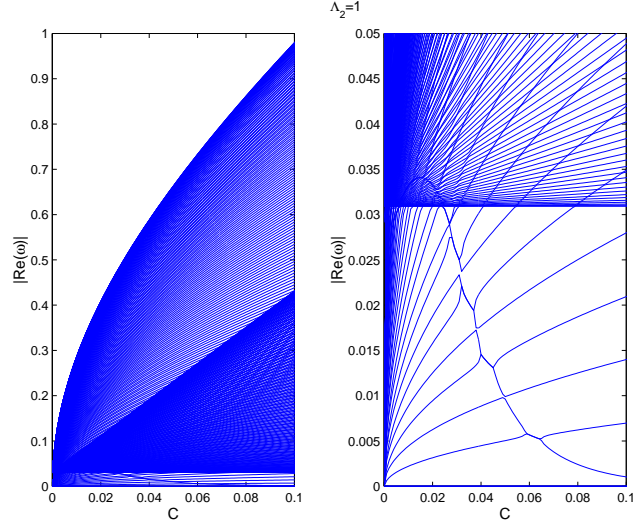
9

Fig. 4. Real part of eigenfrequencies versus coupling C for dark-bright one-soliton solutions with $\Lambda_2 = \Lambda_1 = 1$. The right panel is a zoom of the left panel where the the existence of a Hopf bifurcation cascade is highlighted.
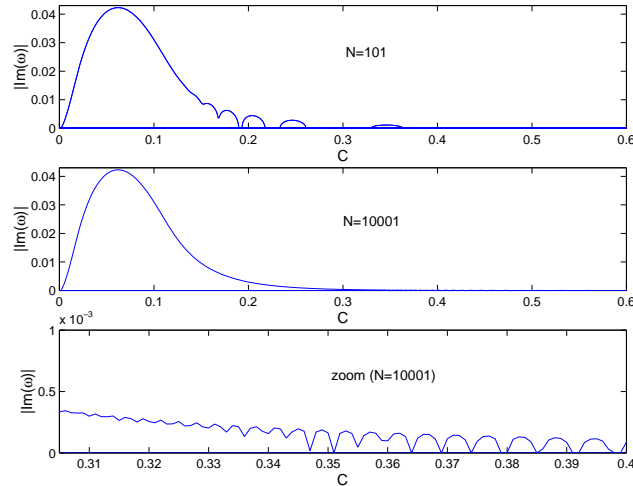

Fig. 5. The imaginary part of the eigenfrequencies is plotted versus the coupling C for $\Lambda_2 = 0.9$. The dependence on the system size is illustrated: $N = 101$ is chosen in the top panel whereas $N = 10001$ is taken in the other ones. The bottom panel highlights a zoom-in of the middle panel into a parametric range where bubbles appear.

unstable for every value of C.

3.2.2 Dark-bright two-soliton solutions

Here we consider both the *in-phase* and *anti-phase* cases.

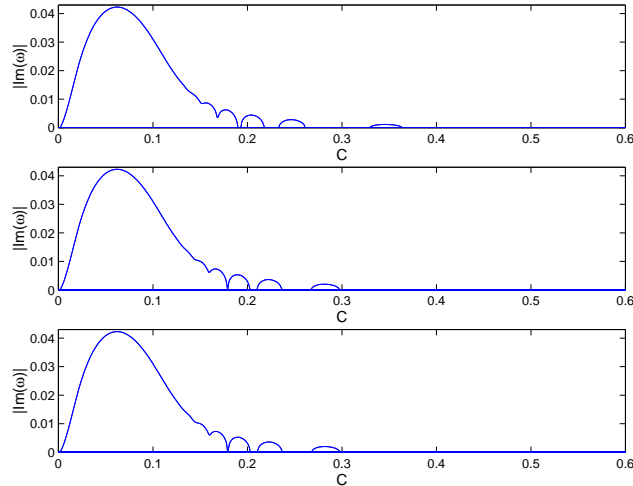In the in-phase case, we observe that the DB solitons behave structurally

Fig. 6. The imaginary part of the eigenfrequencies is plotted versus the coupling C for $\Lambda_2 = 0.9$ and $N = 101$. The (in)dependence of the stability bubbles on the boundary conditions is highlighted. The top panel corresponds to free end boundary conditions, the middle panel to anti-periodic boundary conditions and fixed ends are shown in the bottom panel. Notice that the imaginary parts of the eigenvalues are almost identical for fixed ends and anti-periodic boundary conditions (the differences are $\lesssim 10^{-4}$.)
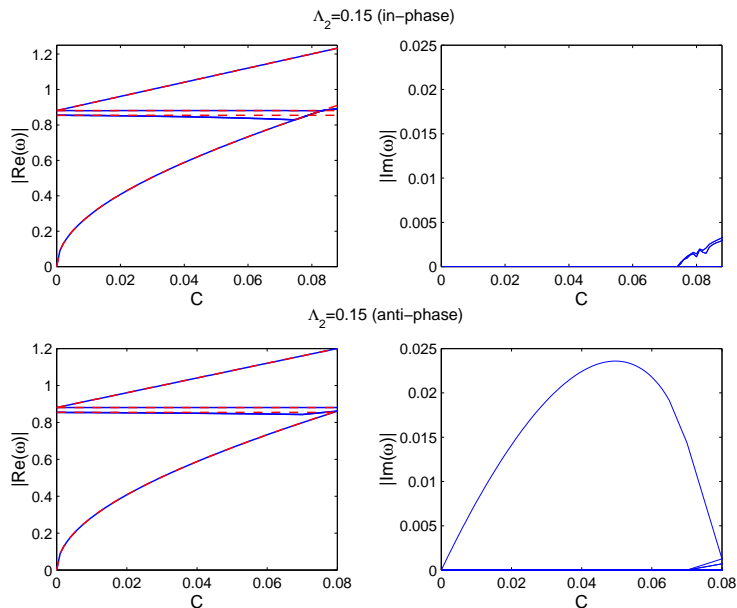

Fig. 7. Real part of the relevant eigenfrequencies (left panels) and imaginary part of the full spectrum (right panels) versus C of the DB two-soliton solutions. Dashed lines in left panels correspond to analytical predictions (12)-(14).

in a similar way to the case of the single dark-bright soliton solutions with $\Lambda_2 \leq 0.51$ (left region of Fig. 2), that is, for small C the solutions are stable up to a critical value where they destabilize, with their bright component disappearing above a second critical value of C; additionally, stability bub-
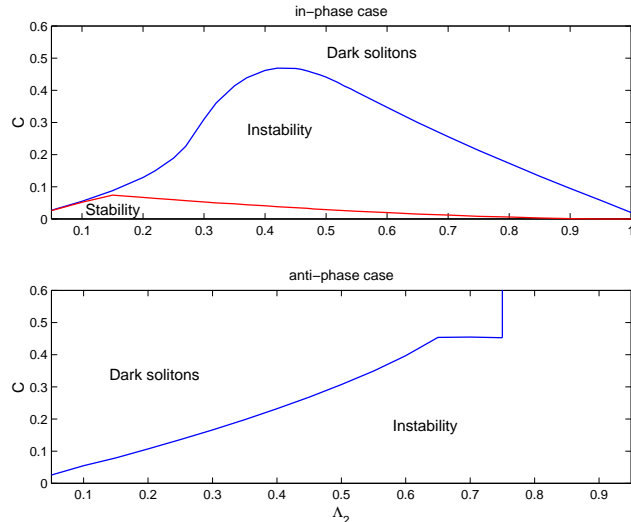
Fig. 8. Existence and stability properties of the dark-bright two-soliton solutions as a function of coupling C and frequency Λ_2, with the fixed value $\Lambda_1 = 1$. The top panel shows the in-phase case, while the bottom one illustrates the anti-phase case.

bles do not exist. Similarly, there do not exist regions where the DB pair solution persists for arbitrary C. The latter is natural to expect since the in-phase structure induces repulsion among the bright components[3]; this fact, combined with the repulsion among the dark components, does not allow the possibility of sustaining stationary such solutions near the continuum limit. Moreover, we observe that the maximum value of C does not depends monotonically with Λ_2, having a maximum around $\Lambda_2 = 0.42$. For Λ_2 below this critical value, and upon increase of C, the bright spot amplitude vanishes similar to the DB 1-S case but now the solution that exists above the critical value of C consists of 2 dark soliton waveforms; however, when Λ_2 is above the critical value, the continuation fails past a certain critical C. This is due to the existence of an inverse Hopf bifurcation, which may be caused by the interaction between the two peaks of the bright component, similarly to what is observed in [36].

On the contrary, the out-of-phase case solutions are *always* exponentially unstable. Additionally, we observe a monotonically increasing behaviour of the maximum value of C with Λ_2 up to $\Lambda_2 \approx 0.65$. In this parametric range, the bright spot vanishes above the critical coupling. On the other hand, for $0.65 \lesssim \Lambda_2 \lesssim 0.75$, the curve is almost horizontal and the solutions experience an inverse Hopf bifurcation. Finally, DB 2-S exist for any value of C whenever

---

[3] This is an important structural characteristic of the self-defocusing nature of our nonlinearity. Namely, contrary to what is standardly known for the case of self-focusing/attractive interactions [1], bright solitons here *repel* when they are *in phase*, but *attract* when they are *out of phase*; cf. also with the continuum case discussion of Ref. [13].
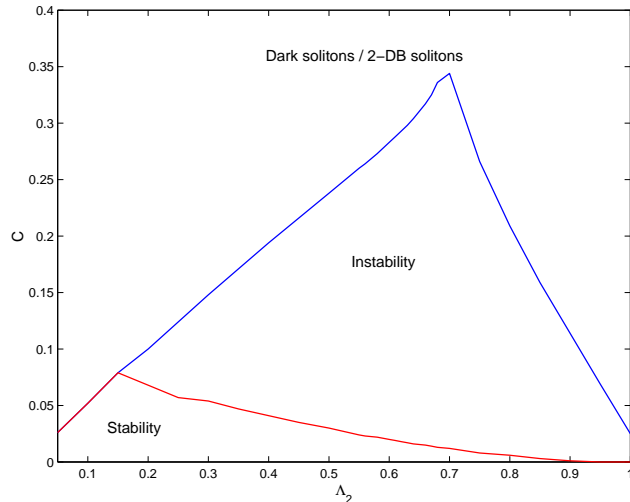
Fig. 9. Existence and stability properties of the dark-bright and dark two-soliton solutions as a function of coupling C and frequency Λ_2, with the fixed value $\Lambda_1 = 1$.

$\Lambda_2 \geq 0.75$. These findings are summarized in Figs. 7 and 8. Let us mention in passing that somewhat surprisingly, the stability for small C is the opposite than for the case of bright solitons which are separated by an even number of sites (i.e. in the latter case, the bright 2-solitons in-phase are unstable for any coupling whereas the bright 2-solitons in anti-phase are stable for small coupling) [36]; for a corresponding discussion in the multi-soliton interactions in the 2d case, see e.g. [37].

3.2.3 Dark-bright and dark two-soliton solutions

The dark-bright and dark two-soliton solutions behave structurally in a similar way to the DB 1-S or DB 2-S in-phase solutions. There are however some important differences. The maximum value of C (as a function of Λ_2) for which such solutions exist has a maximum for $\Lambda_2 = 0.70$. Below this value, the amplitude of $v_1 < 0$ (i.e. the amplitude of the absent bright spot), increases its absolute value, and, above the maximum C the DB+D soliton transform into a DB 2-soliton solution in anti-phase. For $\Lambda_2 > 0.70$, the soliton experiences an inverse Hopf bifurcation at the critical C. Figure 9 illustrates the existence and stability properties of the dark-bright and dark two-soliton solutions as a function of the coupling C and the frequency Λ_2.

3.2.4 Summary of existence and stability results

The previous findings for dark-bright two-soliton solutions and for the dark-bright and dark two-soliton pair solutions were obtained for a separation of two sites between holes or peaks. However, the results are similar when the separation increases up to 3 sites. The relevant effects on the lattice decay

13

exponentially with the separation, so that for large values of this separation, the DB structures behave as isolated ones and the stability properties are similar to the dark-bright one-soliton solutions.

Arguably, the most interesting of the above results concerns the stability of the DB two-soliton state and especially the independence of this result on the distance between the DB waves; instead, the result seems to solely (and *critically*) depend on the relative phase of the bright components. It is relevant to contra-distinct this to the case of simply two-dark solitons of the form defined above which would be stable (at least close to the AC limit) independently on the distance d, and also to the case of two bright *gap* solitons, considered before in [38] (see also [33]) whose stability would depend on *both* the distance d and the relative phase. In fact, in the latter case of two bright gap solitons for defocusing nonlinearities, using the so-called staggering transformation to convert the defocusing dynamics into focusing one, it is straightforward to establish [38] that in-phase excited sites, separated by an even number of sites are unstable, while by an odd number of sites are stable (for small C), while the situation is reversed for anti-phase excitations (stable for an even site distance and unstable for an odd one). On the other hand, here we observe that the "dressing" of the interaction of the bright components via their dark partners leads to stability for in-phase excitations and instability for out-of-phase ones. At a qualitative level, one can present the following straightforward argument towards understanding this effect: it is well-known (see also the discussion below regarding DB soliton collisions) that DB solitons with in-phase bright components *repel* each other while DB states with out-of-phase bright excitations attract each other; see e.g. the fundamental experimental work of [5], and the very recent theoretical discussion of [39]. As a result the state with out-of-phase bright excitation will be structurally less robust e.g. if the DB pair is moved closer, the attraction becomes stronger and the tendency is to deviate further from the equilibrium. If the pair is moved further away, the attraction becomes weaker, and again the further deviation from equilibrium is favored. The contrary is true for the in-phase excitation. The repulsion of the bright components, if they are brought closer or drift away from the equilibrium, favors in both cases their return to equilibrium indicating its structural robustness.

4 Collisions

Having examined the stability of the DB soliton configurations, we now turn to a more systematic examination of collision events involving two DB waves or a dark-bright and a dark one. All the numerical computations below have been performed perturbing only the bright parts of the corresponding solutions. In the case of dark-bright and dark two-soliton pairs, the perturbation

14

only affects the single bright spot, and for the other cases the perturbations affect symmetrically each bright wavepacket so that they can move in opposite directions. For most of the collisions we have taken $N = 402$, $\Lambda_1 = 1$, $\Lambda_2 = 0.7$ and for each value of C, the values of α (the parameter controlling the "kick" $\propto e^{i\alpha(n-n_0)}$, where n_0 is the center of the soliton), have been taken in the interval $[0.01, 0.30]$. The velocity of the dark-bright soliton increases when α increases. The solitons are initially separated by a distance of 200 lattice sites. Notice that only collisions at intermediate and high values of C have been considered, as for low values of C the solitons are not mobile due to discreteness effects which impede their traveling. We have observed that, for $\Lambda_2 = 0.7$, which is the case analyzed in most of the cases below, C must be higher than 1.2 if $\alpha = 0.01$ and 0.9 if $\alpha = 0.3$. The critical coupling needed for mobility decreases with Λ_2 and α.

4.1   Collisions between a dark-bright and a dark soliton

(1) *Collisions at intermediate coupling*

First of all, we consider collisions for $C = 1.23$. The possible outcomes of such events are illustrated in Figs. 10-11, obtained with increasing values of α. This value of C has been chosen so that it is "intermediate" between the small coupling regime (of low soliton mobility) and the high coupling regime where the collisions are essentially tantamount to the ones in the continuum model (and discreteness is irrelevant). In this intermediate range, the discreteness plays a crucial role in determining the collisional outcome and provides a rich variety of potential scenarios. The collision events are illustrated by means of space-time diagrams representing the contour plots of the densities of the two fields, $\{|u_n|^2\}$ and $\{|v_n|^2\}$, respectively.

For α small enough the static dark remains at rest after the collision, and the dark-bright is reflected from it, as shown in Fig. 10 for $\alpha = 0.08$. For larger values of α such as 0.12 of the middle panel of Fig. 10, the dark-bright may rebound but also concurrently leads to the motion alongside it of the stationary dark soliton, formulating an interesting co-propagating dark-bright and dark soliton pair. This apparent effect of discreteness is not only absent for higher couplings C (as we will see below), but also is especially unexpected given the apparently repulsive nature of the interaction between the dark-bright and the dark soliton for large C (i.e., in the continuum limit), discussed below. This scenario appears for a small interval of α values. The explanation that we offer for this effect is the following: for the present value of C and the relevant lattice size $N = 402$, the dark soliton is, in fact, *dynamically unstable*. While this instability does not manifest itself until the collision event, the latter appears to *trigger* the instability by providing a significant perturbation to the stationary dark soliton. As a result, after the collision the dark

15

soliton becomes subject to the oscillatory instability, in turn giving rise (as observed previously) to its motion; see also [40].

For increasing values of α the static dark always gets into motion but some different scenarios appear:

(a) The dark-bright solitary wave rebounds launching out away the static dark, as illustrated for $\alpha = 0.13$ in Fig. 10.

(b) The dark-bright wave may remain nearly stopped, as for $\alpha = 0.24$ in the left panel of Fig. 11.

(c) The dark-bright may continue traveling along the incident direction, as the dark (initially stationary) soliton does; an example of this for $\alpha = 0.245$ can be found in the middle panel of Fig. 11.

(d) Lastly, we observe another unusual dynamical scenario unfold in the right panel of Fig. 11: here, apparently the dynamical instability of the stationary dark soliton manifests itself prior to the arrival of the DB soliton (and the ensuing collision event). As a result, after the collision the dark-bright continues traveling without essentially changing its velocity while the dynamically unstable dark soliton continues traveling in the opposite direction.
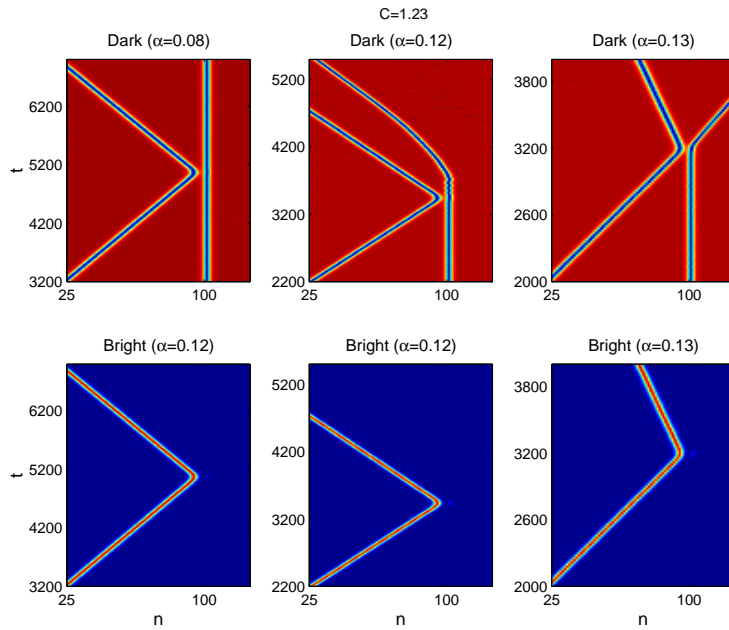

Fig. 10. Three dark-bright+dark 2-S collisions corresponding to increasing values of α; $\alpha = 0.08$ on the left, $\alpha = 0.12$ in the middle and $\alpha = 0.13$ on the right. Relevant parameters are chosen as: $C = 1.23$; $\Lambda_1 = 1$; $\Lambda_2 = 0.7$.

(2) *Collisions at higher coupling*

Some prototypical examples of collisions at higher coupling are also given for $C = 3$ in Fig. 12. These are essentially for a regime where discreteness is irrelevant and the dynamics chiefly represents the near-elastic collisions of the continuum limit (which, however, can still be fairly complex, exhibiting beating and breathing phenomena as illustrated in [41]).
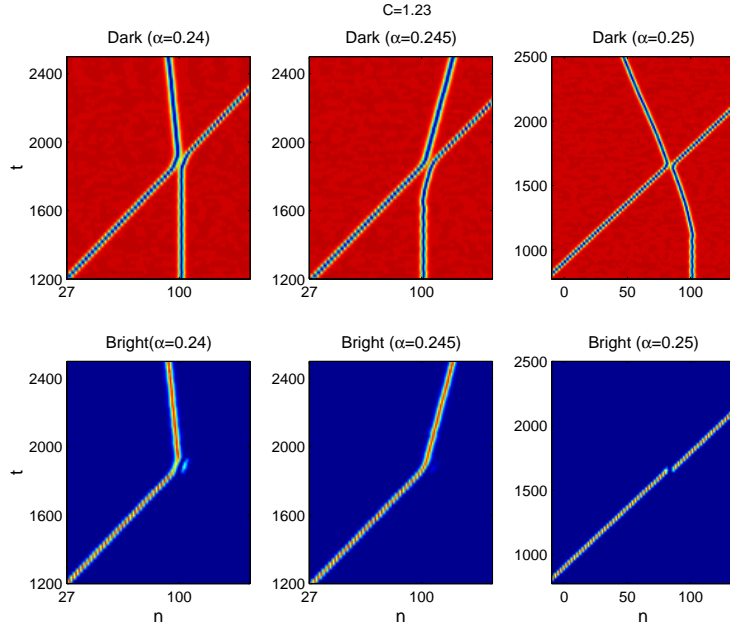
16

Fig. 11. Same as Fig.10, but for larger values of the initial kick α (0.24, 0.245 and 0.25, respectively on the left, middle and right), corresponding to larger speeds.

Nevertheless, we show them here to showcase the repulsive nature of the interaction between the dark-bright and the dark soliton. It is clear that the low velocity collision of the left panel of the figure signals a repulsive occurrence whereby the centers of the two solitons never "touch". There is a critical kinetic energy which enables the DB soliton to balance the repulsion induced from the stationary dark soliton. Close to this critical point, there is a prolonged merger of the two waves, prior to their separation as evident in the middle panel of the figure. Finally, the right panel shows a supercritical case, where the DB soliton possesses enough kinetic energy to *overcome* the repulsive barrier posed by the dark stationary state. In that case, the dark remains stationary, while the dark-bright passes through it. It should be noted that in these events, the large value of C mitigates the dynamical instability (which now has a very small growth rate as the continuum limit is approached), hence some of the more elaborate occurrences of Figs. 10-11 are absent here.

4.2 Two dark bright solitons collisions

In order to observe the collision scenario between two DB solitons, we fix $C = 1.55$. This value of C has been chosen so that it is "intermediate", as in the above examined collisions between a dark-bright and a dark soliton.

First of all, we consider slow soliton collisions. The parameter α should be small enough so that the kinetic energy does not overwhelm the details of the
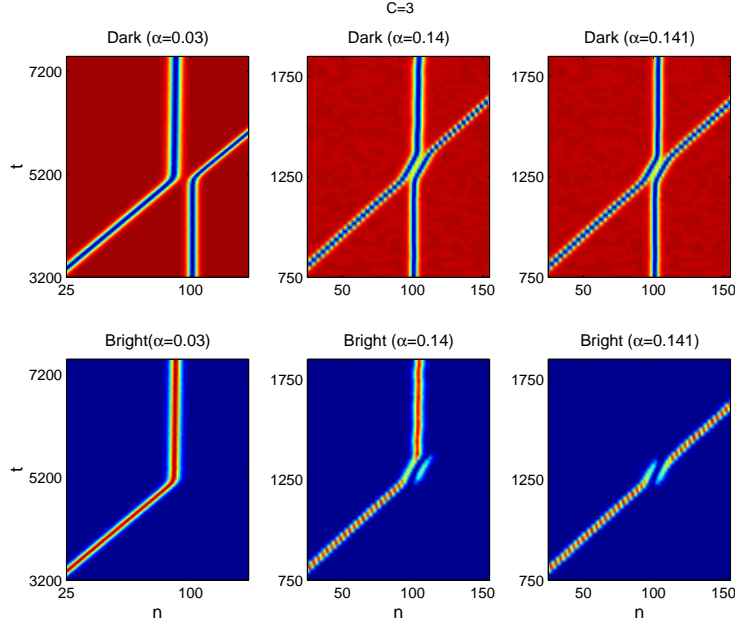
17

Fig. 12. Dark-bright and dark solitary wave collisions corresponding to increasing values of α; $\alpha = 0.03$, 0.14 and 0.141, respectively for the left, middle and right panels. Other parameters are chosen as $C = 3$; $\Lambda_1 = 1$; $\Lambda_2 = 0.7$.

collisions. For these low velocities dark-bright solitons with in-phase bright components *repel* each other while dark-bright solitons with out-of-phase bright excitations attract each other. These results agree with the experimental work of [5] and the theoretical work of [13] which discusses the nature of the inter-action.
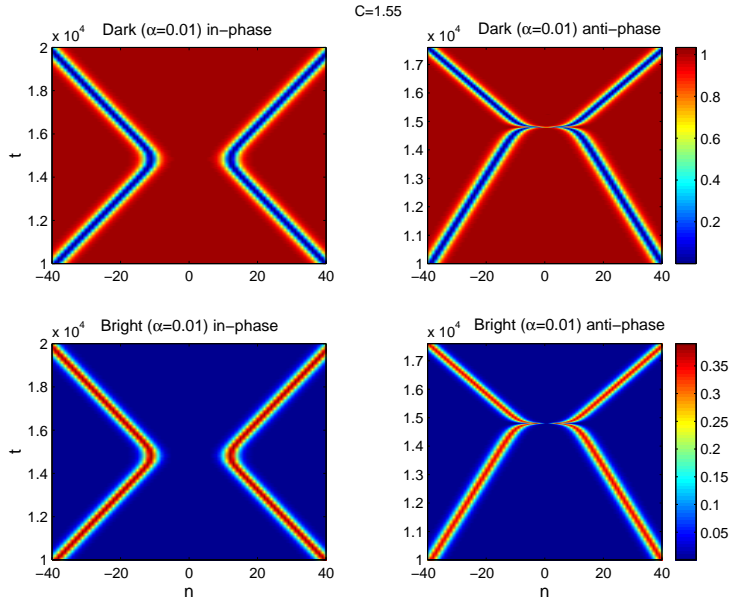

Fig. 13. An example of dark-bright two-soliton collisions. (Left): in-phase case. (Right): anti-phase case. Parameters: $C = 1.55$; $\Lambda_1 = 1$; $\Lambda_2 = 0.7$ and $\alpha = 0.01$.

18

As an example, taking $\alpha = 0.01$, Fig. 13 illustrates a dark-bright two-soliton collision event for the in-phase case (left column) and for the anti-phase case (right column), with $\Lambda_2 = 0.7$. We observe repulsion of the dark components when the bright components are in phase and attraction when they are out of phase.

If the velocity is increased, the following modifications are observed. On the one hand, in the in-phase bright component case, the repulsion of both the dark and bright components is mitigated by the increase of kinetic energy (i.e., the turning points of the relative motion occur closer to $n = 0$); on the other hand, for the anti-phase bright component, the kinetic energy and attractive interaction cooperate in bringing the solitons together. Fig. 14 shows an example of the outcome of both cases for $\alpha = 0.3$.
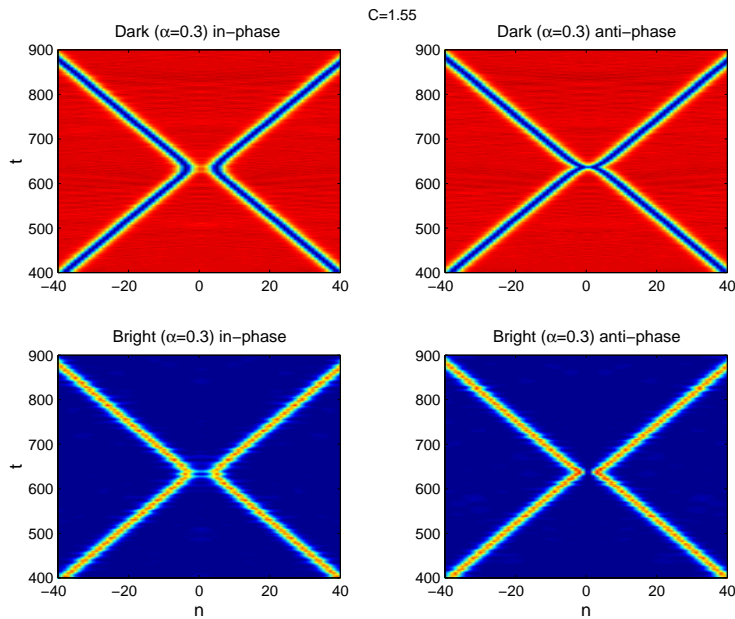

Fig. 14. Same as Fig. 13, but for $\alpha = 0.3$ that corresponds to a larger speed.

In order to discern if the dark components of the two DBs with π out of phase bright components cross each other or not, we have traced in Fig. 15 the dark component density profile $|u_n|^2$ at the time where both colliding solitons are at the minimum distance for the right panels of Figs. 13 and 14. We can observe the existence of two dips instead of a single one, which is a clear indication that the dark components of the solitons do not cross each other. In fact, as discussed also in [42], it is only when the two dark soliton centers coincide that they pass through each other (i.e., that they overcome the finite barrier of repulsion between them).

Ref. [13] considers the interaction between two DBs with π out of phase bright components as the norm of the bright component is modified. There, the fading attraction effect between the bright components (as their norm decreases)
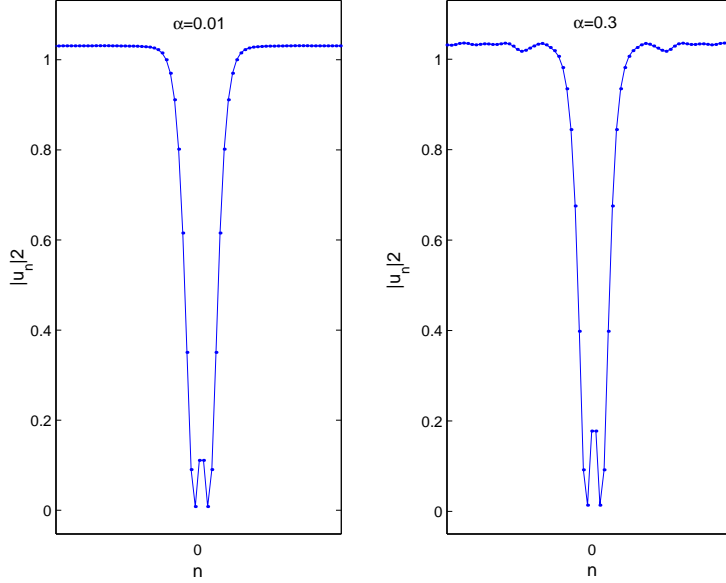
Fig. 15. Density profile of the dark components of the colliding solitons of right panels of Fig. 13 (left) and Fig. 14 when the distance between them is the shortest.

enables the emergence of a repulsive character of the interaction due to the dark components. In order to check if this phenomenon also occurs in our system, we have performed some simulations varying Λ_2 (increasing Λ_2 is equivalent to increase the norm of the bright component) showing that there is a critical value of Λ_2 below (above) which the dark components repel (attract) each other. This phenomenon is illustrated in Fig. 16.

Finally, we have checked that, contrary to the dark-bright and dark solitary wave collisions, no fundamental qualitative differences are observed when a high coupling in implemented. That is, collisions at intermediate and strong couplings C roughly exhibit the same principal phenomenology (hence, we do not show any of the latter here).

5 Conclusions and Future Challenges

In the present work, we offered a numerical perspective on the existence, stability, dynamics and interactions of single and multiple dark-bright solitons not only between them, but also with dark solitons in the setting of nonlinear dynamical lattices. The presence of discreteness enabled a number of interesting variants to the previously studied continuous setting. Some of these variants could be anticipated on the basis of analogous studies of dark solitons [33]. E.g., the dark-bright single solitons could be stable only up to a critical coupling (although finite-size effects could provide additional stabilization). The same thing would be true for pairs of dark-bright and dark solitons. The collisions
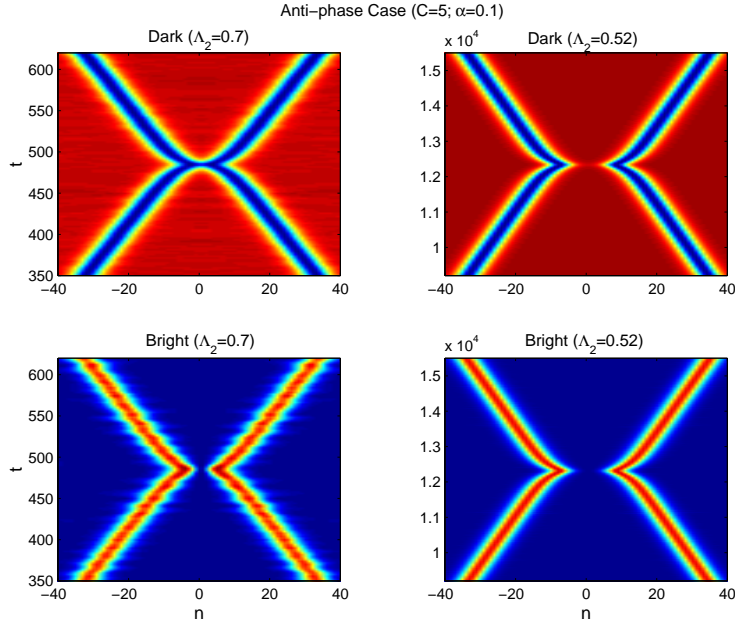
Fig. 16. Comparison between 2 DB soliton collisions when Λ_2 is varied ($\Lambda_2 = 0.7$ on the left, while $\Lambda_2 = 0.52$ on the right; $C = 5$ and $\alpha = 0.1$ in both cases). It is observed that below a critical value, the dark component repulsion can be deemed to be stronger than the anti-phase bright component attraction and hence creates a potential barrier that, in turn, induces a finite separation "turning point" in the interaction between the solitary waves.

of the latter pairs indicate the repulsive interaction between the dark-bright and the dark states. On the other hand, a number of interesting novel features were revealed. Relevant examples include the generic instability of the dark-bright for a sufficiently strong bright component, the generic instability of out-of-phase two-DB soliton pairs, and the generic stability (again for large enough bright component) of in-phase two-DB soliton pairs. Discreteness was also found to play a significant role in affecting collisions for "intermediate" coupling strengths (not too small, so that the excitations would get pinned, nor too large so that they would interact in a quasi-continuum way). There, its potential combination with the dynamical instability e.g. of stationary dark solitons could yield a variety of interesting collisional outcomes, especially in the collisions of dark-bright solitary waves with dark ones.

There are numerous directions in which one can consider expanding the considerations presented herein. One possible example is an analytical attempt to calculate the linearization eigenvalues of two-DB soliton pairs, to explicitly prove the stability conclusions numerically inferred herein (and to obtain some mathematical intuition on these findings). Another possibility from a numerical viewpoint is to extend the considerations presented herein to vortex-bright solitons (or to dark-bright rings) in higher-dimensional settings, by analogy to the continuum form of such symbiotic entities recently considered in [14]. There one can potentially envision situations where the symbiotic structure

may be stable although neither of its constituents is robust by itself. Potential experimental realizations of dark-bright solitons and soliton pairs in waveguide arrays (such as lithium niobate ones) could be an excellent source of testing of the relevant ideas in realistic settings.

Acknowledgments

References

[1] Yu.S. Kivshar and G.P. Agrawal, *Optical solitons: from fibers to photonic crystals*, Academic Press (San Diego, 2003).

[2] P. G. Kevrekidis, D. J. Frantzeskakis, and R. Carretero-González, *Emergent Nonlinear Phenomena in Bose-Einstein Condensates*, Springer-Verlag (Berlin, 2008).

[3] Yu.S. Kivshar and B. Luther-Davies, Phys. Rep. **298**, 82 (1998).

[4] Z. Chen, M. Segev, T.H. Coskun, D.N. Christodoulides, Yu.S. Kivshar and V.V. Afanasjev, Opt. Lett. **21**, 1821 (1996).

[5] E.A. Ostrovskaya, Yu.S. Kivshar, Z. Chen and M. Segev, Opt. Lett. **24**, 327 (1999).

[6] Y.S. Kivshar, D. Anderson, A. Höök, M. Lisak, A.A. Afanasjev and V.N. Serkin, Phys. Scripta **44**, 195 (1991).

[7] C.J. Myatt, E. A. Burt, R. W. Ghrist, E. A. Cornell, and C. E. Wieman Phys. Rev. Lett. **78**, 586 (1997).

[8] D. S. Hall, M. R. Matthews, J. R. Ensher, C. E. Wieman, and E. A. Cornell Phys. Rev. Lett. **81**, 1539 (1998).

[9] D.M. Stamper-Kurn, M. R. Andrews, A. P. Chikkatur, S. Inouye, H.-J. Miesner, J. Stenger, and W. Ketterle, Phys. Rev. Lett. **80**, 2027 (1998).

[10] Th. Busch and J.R. Anglin, Phys. Rev. Lett. **87**, 010401 (2001).

[11] H.E. Nistazakis, D.J. Frantzeskakis, P.G. Kevrekidis, B.A. Malomed and R. Carretero-González, Phys. Rev. A **77**, 033612 (2008).

[12] S. Rajendran, P. Muruganandam, M. Lakshmanan, J. Phys. B **42**, 145307 (2009).

[13] C. Yin, N.G. Berloff, V.M. Pérez-García, V.A. Brazhnyi and H. Michinel, arXiv:1003.4617

[14] K.J.H. Law, P.G. Kevrekidis and L.S. Tuckerman, Phys. Rev. Lett. **105**, 160405 (2010).

[15] C. Becker, S. Stellmer, P. Soltan-Panahi, S. Dörscher, M. Baumert, E.-M. Richter, J. Kronjäger, K. Bongs, and K. Sengstock, Nature Phys. **4**, 496 (2008).

[16] C. Hamner, J.J. Chang, P. Engels, M. A. Hoefer, arXiv:1005.2610.

[17] S. Middelkamp, J.J. Chang, C. Hamner, R. Carretero-Gonzalez, P.G. Kevrekidis, V. Achilleos, D.J. Frantzeskakis, P. Schmelcher, P. Engels, arXiv:1005.3789.

[18] N. K. Efremidis, S. Sears, D. N. Christodoulides, J. W. Fleischer, and M. Segev Phys. Rev. E **66**, 46602 (2002).

[19] J. W. Fleischer, M. Segev, N. K. Efremidis, and D. N. Christodoulides, Nature **422**, 147 (2003).

[20] J. W. Fleischer, T. Carmon, M. Segev, N. K. Efremidis, and D. N. Christodoulides, Phys. Rev. Lett. **90**, 23902 (2003).

[21] F. Lederer, G.I. Stegeman, D.N. Christodoulides, G. Assanto, M. Segev and Y. Silberberg, Phys. Rep. **463**, 1 (2008).

[22] S. Flach and A.V. Gorbach, Phys. Rep. **467**, 1 (2008).

[23] H.S. Eisenberg, Y. Silberberg, R. Morandotti, A. R. Boyd and J. S. Aitchison, Phys. Rev. Lett. **81**, 3383 (1998).

[24] D. N. Christodoulides, F. Lederer, and Y. Silberberg, Nature **424**, 817 (2003).

[25] A. A. Sukhorukov, Yu. S. Kivshar, H. S. Eisenberg, and Y. Silberberg, IEEE J. Quant. Elect. **39**, 31 (2003).

[26] I. Bloch, Nature Phys. **1**, 23 (2005).

[27] V. A. Brazhnyi and V. V. Konotop, Mod. Phys. Lett. B **18**, 627 (2004); P. G. Kevrekidis and D. J. Frantzeskakis, Mod. Phys. Lett. B **18**, 173 (2004).

[28] O. Morsch and M. Oberthaler, Rev. Mod. Phys. **78**, 179 (2006).

[29] R. Morandotti, H. S. Eisenberg, Y. Silberberg, M. Sorel, and J. S. Aitchison, Phys. Rev. Lett. **86**, 3296 (2001).

[30] E. Smirnov, C. E. Rütter, M. Stepić, D. Kip, and V. Shandarov, Phys. Rev. E **74**, 065601 (2006).

[31] J. Meier, J. Hudock, D.N. Christodoulides, G. Stegeman, Y. Silberberg, R. Morandotti, and J. S. Aitchison, Phys. Rev. Lett. **91**, 143907 (2003).

[32] R.S. MacKay and S. Aubry, Nonlinearity **7**, 1623 (1994).

[33] P.G. Kevrekidis, *The discrete nonlinear Schrödinger equation: mathematical analysis, numerical computations and physical perspectives*, Springer-Verlag (Heidelberg, 2009).

[34] J. Cuevas, Q.E. Hoq, H. Susanto, and P. G. Kevrekidis. Physica D **238**, 2216 (2009); J. Cuevas, G. James, P.G. Kevrekidis and K.J.H. Law. Physica D **238**, 1422 (2009).

[35] M. Johansson and Yu.S. Kivshar, Phys. Rev. Lett. **82**, 85 (1999).

[36] J. Cuevas, B.A. Malomed, D.J. Frantzeskakis and P.G. Kevrekidis. Physica D **238**, 67 (2009).

[37] P.G. Kevrekidis, B.A. Malomed and A.R. Bishop, J. Phys. A: Math. Gen. **34**, 9615 (2001).

[38] P. G. Kevrekidis, H. Susanto, and Z. Chen, Phys. Rev. E **74**, 066606 (2006).

[39] V.A. Brazhnyi and V.M. Pérez-García, arXiv:1004.3672.

[40] Yu.S. Kivshar, W. Królikowski and O.A. Chubykalo, Phys. Rev. E **50**, 5020 (1994).

[41] R. Radhakrishnan and K. Aravinthan, J. Phys. A: Math. Theor. **40**, 13023 (2007).

[42] R.N. Thurston and A.M. Weiner, J. Opt. Soc. Am. B **8**, 471 (1991).